APPENDIX

Appendix A

3.1A X-ray photoelectron spectroscopy of magnetite NPs-

The high-resolution C1s, O1s, and Fe 2p XPS spectra of IO@S and IO@T samples are shown in **figure 3.1A**. The C1s spectrum of IO@S shows in **figure 3.1A (a)** depict two peaks at 284.8 and 288.4 eV, attributed to carbon in C-C/C-H and COO^-/COOH groups respectively both from stearate [1]. The O1s spectrum in **figure 3.1A (b)** exhibit two peaks centered at 532.5 and 530.9 eV corresponding to COO^-/COOH with possible contributions from hydroxidic species and the oxidic O in Fe_3O_4 respectively [2-3]. **Figure 3.1A (c)** shows the presence of Fe ($Fe^{2+/3+}$ $2p_{3/2}$ ~ 710 - 715 eV / $Fe^{2+/3+}$ $2p_{1/2}$ ~ 724 - 727 eV) [4].

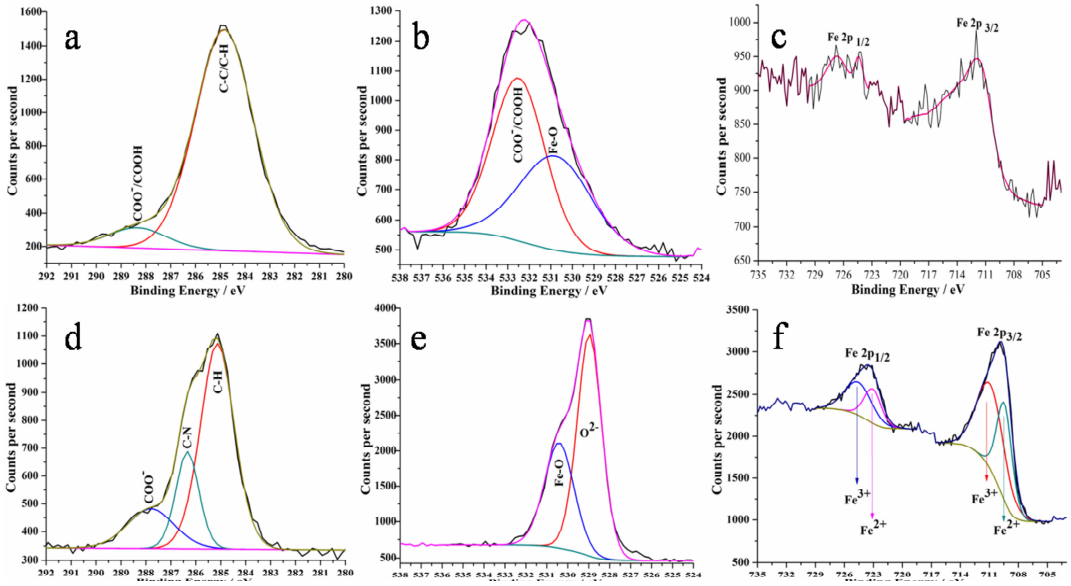

Figure 3.1A High-resolution XPS spectra of magnetite NPs. The a, b, c (IO@S) and d, e, f (IO@T) are the C1s, O1s and Fe2p spectra, respectively.

Figure 3.1A (d) shows the C1s spectrum of IO@T consisting of 285.1, 286.3 and 287.8 eV peaks due to aliphatic C, N-bound C and carboxylic C, respectively. The presence of aliphatic and carboxylic C is indicative of the presence of residual stearate. The O1s spectrum shows the presence of peaks at 529.0 and 530.4 corresponding to lattice oxygen (O^{2-}) and oxidic O in Fe_3O_4. **Figure 3.1A** (f) shows again the presence of typical magnetite signature (Fe^{3+} $2p_{3/2}$ / Fe^{3+} $2p_{1/2}$: 711.2 / 724.7 eV; Fe^{2+} $2p_{3/2}$ / Fe^{2+}

$2p_{1/2}$: 709.5 / 723.2 eV) in both Fe $2p_{3/2}$ and Fe $2p_{1/2}$ regions [3]. It is worthwhile to mention that both in IO@S and IO@T, the binding energy difference between Fe $2p_{3/2}$ and Fe $2p_{1/2}$ is ~ 13.1 eV, confirming retention of the magnetite phase after TMAOH treatment. The absence of satellite peak, which usually emerges around 718.0 eV, is indicative of the absence of any other iron oxide phase in both the spectra. The higher intensity of the Fe 2p peaks compared to C1s shows that the organic layer around IO@T is substantially thinner than at IO@S.

3.2A Magnetization of FePt-B MNPs –

The FePt-B MNPs exhibits less saturation magnetization as compared with FePt-A MNPs. **Figure 3.2A** depicts the magnetization characterization of FePt-B MNPs. The FePt-B MNPs exhibits less saturation magnetization as compared to FePt-A MNPs (**figure 3.2A a-c**). From XRD pattern analysis, it is evident that the crystallinity of FePt-A is higher than FePt-B which can be correlated to the observed enhanced saturation magnetization. The observed reduction in saturation magnetization may also be assigned to the surface dead layer effect [5]. The broader ZFC magnetization curve of FePt-B MNPs (**figure 3.2A d**) can be assigned to broad particle size distribution. It is also observed that the coercivity increases with decreasing temperature and attains the maximum at 25 K in FePt-A and B MNPs. The increased coercivity is the result of increased anisotropy energy barriers with decreasing temperatures.

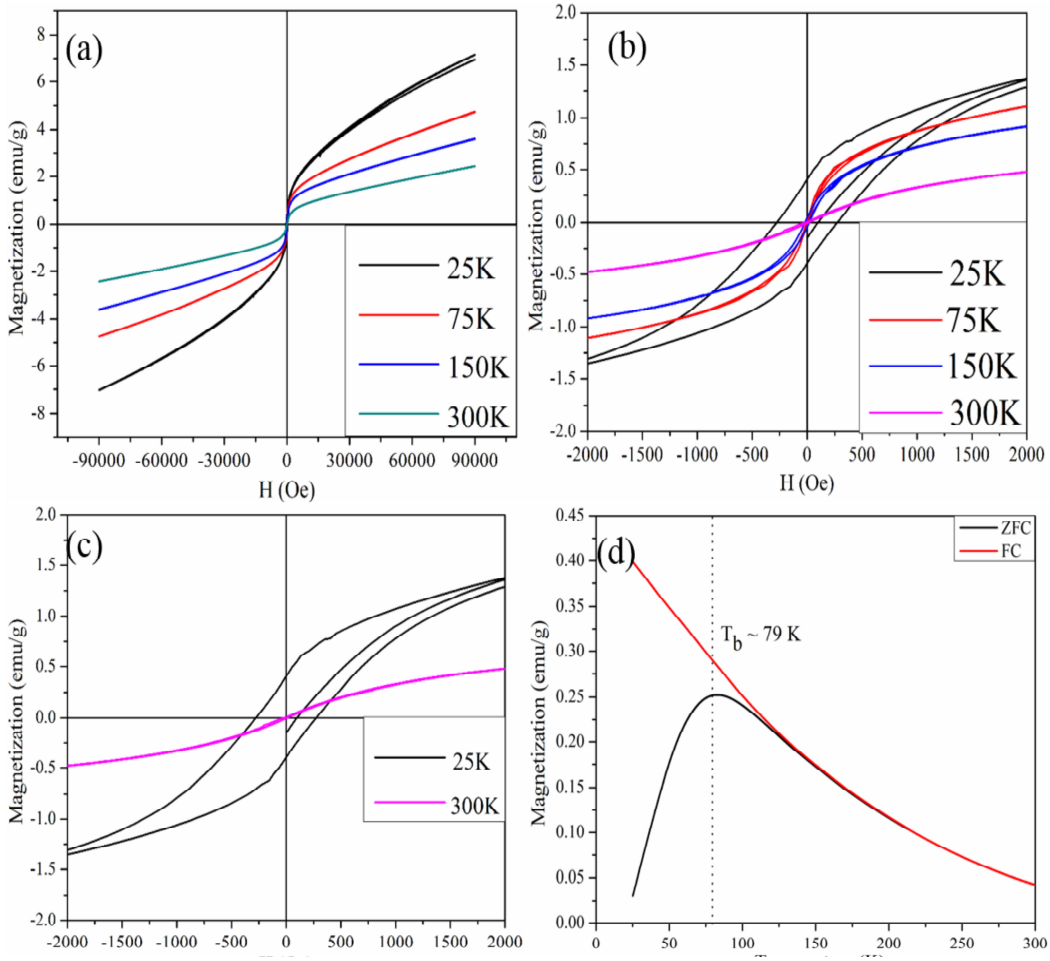

Figure 3.2A The magnetization characterization of FePt-B MNPs (a and b) M-H curves at different temperatures of as prepared FePt-B MNPs, (c) M-H curves at room temperatures and 25K of as prepared FePt-B MNPs and (d) magnetization versus temperature curve measured under ZFC and FC condition.

3.3A Toxicity assay of FePt-A MNPs –

For quantifying *in vitro* cell viability with FePt-A MNPs, Resazurin Reduction Assay or Alamar Blue (AB) toxicity assay was performed [6, 7]. AB toxicity assay has been considered superior to other classical assays for cell viability because its reagent is extremely stable, water soluble, non-toxic to the cells and continuous monitoring of cultures is possible with time. The detailed toxicity procedure is given in Chapter 4. The concentration of FePt-A stock solutions used in the experiment was 0.01535 mg/mL. Dose-dependent concentrations of FePt-A systems are put in **table-1A**.

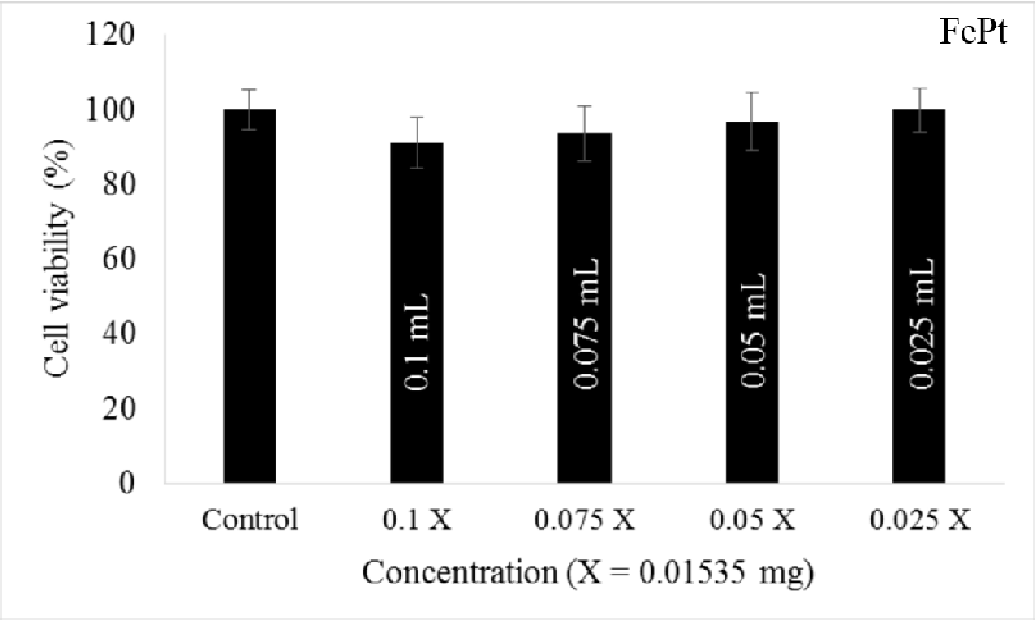

Figure 3.3A - Viability of RAW 264.7 macrophage cell line compared to control indicated by AB assay when the cells were exposed to TGA capped FePt-A MNPs.

The % cell viability of control is taken as reference for calculation of cell viability with samples. From the graph, it is seen that the viability of RAW 264.7 macrophage cell lines is not affected (< 80 %) by FePt-A MNPs even at 0.1 mL concentration.

Table 1A Dose-dependent concentration of FePt-A MNPs

Si. no.	Sample	Concentration (Stock)	Volume	Dose dependent concentration
1	FePt-A	0.01535 mg / mL	0.1 mL	0.001535 mg
			0.075 mL	0.001151 mg
			0.05 mL	0.000767 mg
			0.025 mL	0.000383 mg

It is also observed that when the dose of FePt-A was decreased i.e. when the volume of test sample decreases, the viability of the cell increases. It represents good biocompatibility with RAW 264.7 macrophage cell line.

References:

1. Lee, W. H. *et al.* X-ray photoelectron spectroscopic studies of surface modified single-walled carbon nanotube material. *Appl. Surf. Sci.* **181,** (1), 121--127, 2001.

2. Briggs, D. & Beamson, G. XPS studies of the oxygen 1s and 2s levels in a wide range of functional polymers. *Anal. Chem.* **65,** (11),1517--1523, 1993.

3. Durdureanu-Angheluta, A. *et al.* Progress in the synthesis and characterization of magnetite nanoparticles with amino groups on the surface. *J. Magn. Magn. Mater.* **324,** (9), 1679--1689, 2012.

4. Wang, Z. Zhu, *et al.* One-pot green synthesis of biocompatible arginine-stabilized magnetic nanoparticles. *Nanotechnology* **20,** (46), 465606--465615, 2009.

5. Tanaka, Y. *et al.* Influence of surface ligands on saturation magnetization of FePt nanoparticles. *Appl. Phys. Lett.* **92,** (9), 093117--093119, 2008.

6. Bonnier, F. *et al.* Cell viability assessment using the Alamar blue assay: A comparison of 2D and 3D cell culture models. *Toxicol. Vitr.* **29,** (1), 124--131, 2015.

7. Cumming, G. *et al.* Error bars in experimental biology. *Journal of Cell Biology* **177,** (1), 7--11, 2007.

Appendix B

4.1A XRD deconvolution of CdTe and CdSe

Both the major peaks of CdTe and CdSe have been deconvoluted with Gaussian fitting. Deconvolutions show the presence of CdS in both systems.

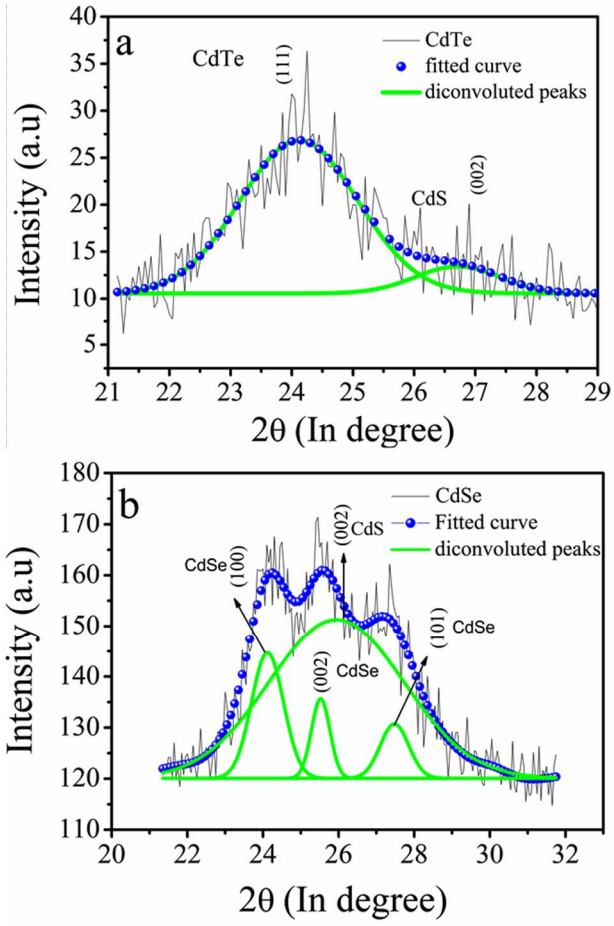

Figure 4.1A Deconvoluted XRD patterns of (a) CdTe and (b) CdSe QDs systems.

4.1B *In vitro* bright field and fluorescence images of control

After Alamar Blue (AB) assay, cells are taken for imaging. These cells contain reduced from of resazurin, known as resorufin. It will show fluorescence when it is excited at a wavelength 530 nm. Images were taken by Leica trinocular inverted research microscope (Leica DMI 6000 B) with 63X oil-immersion objective lens.

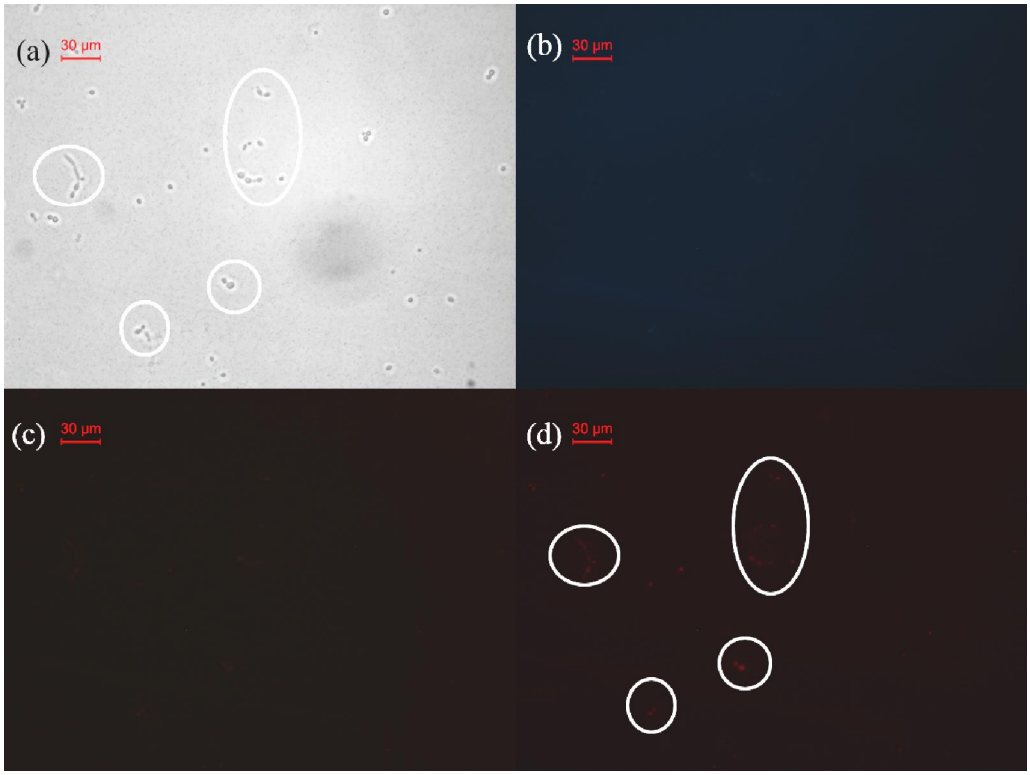

Figure 4.1B - *In vitro* bright field and fluorescence images of control has RAW 264.7 macrophage cells and media. Images have taken by fluorescence microscope under (a) bright field and at an excitation wavelength of (b) UV (c) blue and (d) green light. Position of the marked circles in a figure (d) indicates fluorescence cell at green excitation.

In imaging process, the samples were excited at UV, blue and green lights and their wavelengths (ƛ) corresponds to 360, 450 and 530 nm respectively for examining its morphology and fluorescence property (refer **figure 4.1B**). There is no fluorescence image using UV and blue excitation whereas the green light excited a little fluorescence image have observed.